Submitted to The
Physical Review A

LBL-903
Preprint

QUENCHING OF THE 2^1S_0 METASTABLE STATE OF HELIUM BY AN ELECTRIC FIELD

Charles E. Johnson

September 1972

AEC Contract No. W-7405-eng-48

LBL-903

Submitted to The Physical Review A LBL-903

Quenching of the 2^1S_0 Metastable State of Helium By An Electric Field*

Charles E. Johnson
University of California
Lawrence Berkeley Laboratory, Berkeley, California 94720

September 1972

ABSTRACT

A time-of-flight technique has been used to measure the quenching of the 2^1S_0 metastable state of helium by a static electric field. Neutral, ground-state helium atoms effusing from a cooled source slit are immediately excited to the 2^1S_0 and 2^3S_1 metastable states by a pulse of antiparallel, magnetically focused electrons. The metastable beam is collimated before passing through a uniform electric field region 0.5-m long and is then preferentially detected at the end of the time-of-flight region, 1.825 m from the electron gun. The time-of-flight distribution for the 2^1S_0 state is separated from that of the 2^3S_1 state by illuminating the beam before the electric field region with an rf-discharge helium lamp. The 2^1S_0 state is quenched by resonant absorption of a 20,581-Å photon, raising the atom to the 2^1P_1 state, which then decays to the $^1S_0$ ground state; the 2^3S_1 state remains unaffected because it is the ground state for the triplet system. The 2^1S_0 time-of-flight distribution is therefore obtained from the difference between

the full beam and the quenched beam. The number of 2^1S_0 atoms arriving at the detector in specific velocity intervals with the electric field off is compared to the number with the field on to determine the quenching rate ($= kE^2$). The result for the quenching constant k for both He^3 and He^4 with E in kV/cm is $k = 0.933 \pm 0.005$; this value is in good agreement with theory and with an earlier, less accurate, experiment. The error in the present experiment arises from a 0.5% uncertainty in the effective length of the electric field region.

I. INTRODUCTION

A time-of-flight technique[1] has been used to measure the quenching of the 2^1S_0 metastable state of helium by a static electric field. The 2^1S_0 state usually decays by spontaneous two-photon emission;[2] however, the presence of a sufficiently strong electric field may, through admixtures of n^1P states, quench the 2^1S_0 state and yield a single photon. This quenching process may be viewed as the zero frequency limit of stimulated two-photon emission.[3]

The theoretical value[4,5] of 19.5 msec for the two-photon radiative lifetime of the 2^1S_0 state of helium is in good agreement with the experimental value of 19.7 ± 1.0 msec. Other helium-like two-photon lifetime measurements[6] in Li^+ and Ar^{16+} are also in good agreement with theory. An additional test of the calculations is provided by a measurement of the quenching rate ($= kE^2$) of the 2^1S_0 state in a static electric field E; as shown in Sec. II, the matrix element used to calculate the quenching constant k is identical to the matrix element required in the calculation of the two-photon decay rate, but with one photon frequency equal zero.

The motional electric field quenching of the $2^2S_{1/2}$ metastable state of Li^{2+}, C^{5+}, and O^{7+} has been measured[7] and then used in conjunction with the Bethe-Lamb theory[8] of quenching to obtain the Lamb shifts of these hydrogen-like heavy ions. However, as previously noted,[9] the Bethe-Lamb theory, although apparently adequate for hydrogen-like systems, predicts a quenching constant for the 2^1S_0 state of helium 25% greater than a time-independent perturbation calculation,[10,11] and the perturbation calculation agrees with an earlier measurement[11] of the 2^1S_0 quenching constant. Thus, an accurate measurement of the quenching constant for the 2^1S_0 state of helium can serve an an independent confirmation of the theory of electric field quenching of a metastable state. Using the Heitler-Ma formalism, Fontana and Lynch[12] have investigated two excited levels coupled by an external perturbation (electric field) and shown that the phenomenological Bethe-Lamb theory is justified in this case. Using a non-perturbative time-dependent approach, Holt and Sellin[13] have obtained a result for three excited levels which reduces to the Bethe-Lamb theory when applied to hydrogen-like systems. For the quenching of the 2^1S_0 state of helium, however, an accurate comparison of theory and experiment requires the treatment of all excited discrete n^1P levels as well as the continuum.

Following a second-order time-dependent perturbation theory of quenching, this paper outlines the time-of-flight technique and apparatus, and then explains the data analysis used to obtain an experimental result for the quenching constant of the 2^1S_0 metastable state of both He^3 and He^4.

II. THEORETICAL DECAY RATE

The use of perturbation theory to calculate the quenching rate of the 2^1S_0 state of helium by a static electric field is sufficient for this experiment, since not only is the applied electric field weak, but also the 2^1S_0 atoms enter and leave the electric field region slowly. In addition, the widths of all levels are small compared to the energy separations. However, the vanishing of all first-order perturbation matrix elements between the 2^1S_0 metastable state and the $^1S_0$ ground state requires the use of second-order perturbation theory. Except for the requirement of second-order, the calculation is analagous to the usual semiclassical derivation[14] of the spontaneous decay rate of an excited state using first-order time-dependent perturbation theory.

The solution of the time-dependent wave equation

$$i \hbar \frac{\partial \psi}{\partial t} = (\mathcal{H}_0 + \mathcal{H}') \psi \qquad (1)$$

is

$$\psi = \sum_n a_n(t) U_n \exp\left(-\frac{iE_n t}{h}\right) ; \qquad (2)$$

U_n is the n^{th} time-independent eigenfunction of the unperturbed Hamiltonian $\mathcal{H}_0$ whose eigenvalue is E_n. The coefficients $a_n(t)$ are determined from the simultaneous solution of the n differential equations

$$i \hbar \dot{a}_k = \sum_n H'_{kn} a_n e^{i\omega_{kn} t} \qquad (3)$$

where $\hbar\omega_{kn} \equiv E_k - E_n$ and H'_{kn} is the matrix element of the perturbing Hamiltonian $\mathcal{H}'$. Then, a perturbation expansion for $a_n(t)$ gives

$$\dot{a}_k^{(0)} = 0$$
$$i\hbar\, \dot{a}_k^{(s+1)} = \sum_n H'_{kn}\, a_n^{(s)}\, e^{i\omega_{kn}t} \; ; \quad s = 0, 1, 2, \ldots \tag{4}$$

The perturbing Hamiltonian

$$\mathcal{H}' = \mathcal{H}^R e^{i\omega t} + \mathcal{H}^E \tag{5}$$

consists of two parts; $\mathcal{H}^R e^{i\omega t}$ represents the radiation field and leads to the spontaneous two-photon decay of the 2^1S_0 metastable state, while $\mathcal{H}^E = eEz$ is the static electric field perturbation. First considering only $\mathcal{H}^R e^{i\omega t}$ as a perturbation, i.e., electric field = 0, yields the two-photon decay rate of the 2^1S_0 state. If the initial state is m, then the initial condition at time $t = 0$ is $a_k^{(0)} = \delta_{km}$ and thus

$$a_k^{(1)} = -\frac{H^R_{km}}{\hbar}\, \frac{e^{i(\omega_{km}+\omega)t} - 1}{\omega_{km} + \omega} . \tag{6}$$

Since $H^R_{km} \equiv 0$ for the $2S \rightarrow 1S$ transition, second order gives

$$i\hbar\, \dot{a}_k^{(2)} = \sum_n H^R_{kn}\, a_n^{(1)}\, e^{i\omega_{kn}t} \tag{7}$$

and allowing for a different frequency ω' of the second photon

$$\dot{a}_k^{(2)} = \frac{i}{\hbar^2} \sum_n \left\{ \frac{H^R_{kn}\, H^R_{nm}}{\omega_{nm} + \omega} \left(\exp\,[i(\omega_{km} + \omega')t] - \exp\,[i(\omega_{kn} + \omega')t] \right) \right\} . \tag{8}$$

The relation $\omega_{km} \equiv \omega_{kn} + \omega_{nm}$ has been used. The solution is

$$a_k^{(2)} = \frac{1}{\hbar^2} \sum_n \left\{ \frac{H^R_{kn} H^R_{nm}}{\omega_{nm} + \omega} \left(\frac{\exp[i(\omega_{km} + \omega + \omega')t] - 1}{\omega_{km} + \omega + \omega'} - \frac{\exp[i(\omega_{kn} + \omega')t] - 1}{\omega_{kn} + \omega'} \right) \right\}. \tag{9}$$

Therefore, the two-photon decay rate[15] is

$$\gamma_0 = \text{const.} \times \left(\sum_n \frac{H^R_{kn} H^R_{nm}}{\omega_{nm} + \omega} \right)^2 \tag{10}$$

where the summation includes all discrete excited states as well as the continuum. However, if the perturbation is now

$\mathcal{H}^E + \mathcal{H}^R e^{i\omega t}$, then the second-order solution is

$$\begin{aligned} a_k^{(2)} = \frac{1}{\hbar^2} \sum_n \Bigg\{ & \frac{H^E_{kn} H^E_{nm}}{\omega_{nm}} \left(\frac{\exp[i\omega_{km} t] - 1}{\omega_{km}} - \frac{\exp[i\omega_{kn} t] - 1}{\omega_{kn}} \right) \\ & + \frac{H^R_{kn} H^E_{nm}}{\omega_{nm}} \left(\frac{\exp[i(\omega_{km} + \omega')t] - 1}{\omega_{km} + \omega'} - \frac{\exp[i(\omega_{kn} + \omega')t] - 1}{\omega_{kn} + \omega'} \right) \\ & + \frac{H^E_{kn} H^R_{nm}}{\omega_{nm} + \omega} \left(\frac{\exp[i(\omega_{km} + \omega)t] - 1}{\omega_{km} + \omega} - \frac{\exp[i(\omega_{kn} + \omega)t] - 1}{\omega_{kn} + \omega} \right) \\ & + \frac{H^R_{kn} H^R_{nm}}{\omega_{nm} + \omega} \left(\frac{\exp[i(\omega_{km} + \omega + \omega')t] - 1}{\omega_{km} + \omega + \omega'} - \frac{\exp[i(\omega_{kn} + \omega')t] - 1}{\omega_{kn} + \omega'} \right) \Bigg\}. \end{aligned} \tag{11}$$

The first term represents the static electric field acting twice and causes no transitions;[16] the second and third terms give the decay arising from the electric field perturbation; the fourth term is the two-photon decay once again.

Finally, considering the 2^1S_0 metastable state of helium and using the electric dipole approximation for the matrix elements of $\mathcal{H}^R$, only the n^1P states contribute to the matrix elements of either $\mathcal{H}^R$ or $\mathcal{H}^E$ in Eq. (11). Thus, including the appropriate density of final states, the total decay rate of the 2^1S_0 state in the presence of an electric field E in kV/cm is

$$\gamma = \gamma_0 + kE^2 \tag{12a}$$

with

$$k = \frac{2\pi}{3}\alpha^3\nu_0 \left(\frac{E(2S) - E(1S)}{R_\infty}\right)^3 (ea_0)^2 \left(\sum_{n=2}^{\infty} M_n(0)\right)^2 \tag{12b}$$

and

$$M_n(0) = \langle 2^1S|\frac{z}{a_0}|n^1P\rangle\langle n^1P|\frac{z}{a_0}|1^1S\rangle \left(\frac{1}{E(2S) - E(nP)} + \frac{1}{E(1S) - E(nP)}\right) \tag{12c}$$

where $\nu_0 = R_\infty/h$ is the Rydberg frequency, e the electronic charge, a_0 the Bohr radius, and α the fine structure constant; the summation is understood to also include the continuum. The first part of $\sum_n M_n(0)$ can be interpreted as representing the perturbation of the 2^1S_0 state by the electric field, while the second part represents the perterbation of the $^1S_0$ ground state. The matrix element $\sum_n M_n(0)$ is identical to the matrix element required in the calculation of the two-photon decay rate γ_0, but with one photon frequency $\nu = 0$. The value[17] for $\sum_n M_n(0)$ used by Jacobs in his calculation[5] of the two-photon decay rate of the 2^1S_0 state is $\sum_n M_n(0) = -25.70$; therefore $k = 0.931$. An independent calculation[18] by Drake gives $k = 0.932$.

III. TIME-OF-FLIGHT ANALYSIS

The formalism for the time-of-flight technique is first outlined for the general case of a metastable beam passing through an electric field region and containing different metastable states created instantaneously by a pulsed electron beam at a single position. This formalism is then applied to the case of helium, showing how the quenching constant k of the 2^1S_0 metastable state can be determined.

A. General Formalism

The number of atoms in a particular metastable state i with initial velocity distribution $N_o(v,i)$, which arrive at the detector at time t is $N_o(v,i)e^{-\gamma_i t}$; the exponential factor allows for the possibility of decay with either the electric field on or off. If L is the length of the electric field region while D is the total time-of-flight distance, then from Eq. (12a) the effective decay rate is

$$\gamma_i = \gamma_{oi} + \frac{L}{D} k_i E^2 . \qquad (13)$$

The probability of detecting a particular metastable atom depends upon the surface efficiency ε_i of the detector. Although this efficiency should be velocity independent for the thermal velocity range of this experiment, it is not necessarily true that the efficiency is independent of position on the detector surface. The total number N(v) of metastable atoms with velocity v that are counted is therefore obtained not only by summing over the different metastable states i , but also by integrating over the surface of the detector:

$$N(v) = \sum_i \int_{surface} \varepsilon_i N_o(v,i) e^{-\gamma_i t} \, dS \; . \tag{14}$$

Dependence on the details of the detector surface is eliminated by ensuring that the initial velocity distribution $N_o(v,i)$ is uniform across the beam so that each point on the detector surface sees the same velocity distribution. The number of metastable atoms counted with the electric field off is then

$$N_1(v) = \sum_i C_i N_o(v,i) \exp(-\gamma_{oi} t) \tag{15a}$$

and with the electric field on is

$$N_2(v) = \sum_i C_i N_o(v,i) \exp[-(\gamma_{oi} + \frac{L}{D} k_i E^2) t] \tag{15b}$$

where $C_i = \int \varepsilon_i dS$ is a constant efficiency factor of the detector.

A comparison of the number of metastable atoms in the same velocity interval with the electric field on and off allows the determination of the quenching constants k_i , since, with the reasonable assumption that the initial velocity distribution $N_o(v,i)$ is the same for all states i , the ratio

$$R = \frac{N_2(v)}{N_1(v)} = \frac{\sum_i C_i \exp[-(\gamma_{oi} + \frac{L}{D} k_i E^2) t]}{\sum_i C_i \exp[-\gamma_{oi} t]} \tag{16}$$

is independent of this velocity distribution. However, the factors C_i are now modified to contain the initial relative populations of the different metastable states i . If only one metastable state is present in the beam, the ratio becomes simply

$$R = \frac{N_1(v)}{N_1(v)} = \exp(-\frac{L}{D} kE^2 t) \ , \qquad (17)$$

which is also independent of the initial velocity distribution. The natural logarithm of this ratio yields the equation of a straight line whose slope is $-\frac{L}{D} kE^2$.

B. Metastable Helium Analysis

Since the 2^3S_1 level in helium is lower in energy than the 2^1S_0 level, electron bombardment excitation to the 2^1S_0 level necessarily produces atoms in both metastable states. Atoms in the 2^1S_0 state can be almost completely quenched, however, by exciting them with 20,581-Å resonance radiation to the 2^1P_1 state, which subsequently decays preferentially to the $^1S_0$ ground state by emitting 584-Å radiation. Application of Eq. (15a) for the electric field off to the specific case of helium shows that the number of counts at the detector with the lamp also off is

$$N_1(\text{off}) = C(^1S)N_o(^1S)\exp(-\gamma_{01}t) + C(^3S)N_o(^3S)\exp(-\gamma_{03}t). \qquad (18a)$$

If the 20,581-Å quench radiation is not fully effective, then only a certain fraction $f(v)$ of the 2^1S_0 atoms are quenched, where $f(v)$ may depend on the velocity of the atom. Again applying Eq. (15a) but now with the lamp on, gives

$$N_1(\text{on}) = [1-f(v)]C(^1S)N_o(^1S)\exp(-\gamma_{01}t) + C(^3S)N_o(^3S)\exp(-\gamma_{03}t) \qquad (18b)$$

as the number of metastable atoms counted at the detector. The difference between Eqs. (18a) and (18b) is the effective number of

2^1S_0 metastable atoms which are analyzed to determine the quenching constant k :

$$N_1(^1S) \equiv N_1(\text{off}) - N_1(\text{on}) = C(^1S)f(v)N_o(^1S)\exp(-\gamma_{01}t) \ . \qquad (19a)$$

A similar result is obtained for the electric field on:

$$N_2(^1S) = C(^1S)f(v)N_o(^1S)\exp[-(\gamma_{01} + \frac{L}{D} kE^2)t] \ . \qquad (19b)$$

The ratio of the number of atoms counted within the same velocity interval is not only independent of the initial velocity distribution $N_o(v)$, but is also independent of the details of the quenching process as contained in the quenching fraction $f(v)$. The logarithm of this ratio is

$$\ln R \equiv \ln\left[\frac{N_2(^1S)}{N_1(^1S)}\right] = -\frac{L}{D} kE^2 t \ . \qquad (20)$$

The calculation of this ratio for several different velocity intervals of the time-of-flight distribution, combined with a measurement of the two distances L and D , and also the electric field E , allows a determination of the quenching constant k from the slope $\left(= -\frac{L}{D} kE^2\right)$ of a straight line, least-squares fitted to a plot of $\ln R$ versus the time-of-flight t .

IV. APPARATUS

The time-of-flight apparatus is outlined in Fig. 1. The major components in addition to the vacuum system are (a) source, (b) metastabilizer (electron gun), (c) quench lamp, (d) electric field plates, and (e) detector. Cooled helium gas effuses from the source and passes vertically through the metastabilizer where a pulsed, antiparallel electron beam excites the ground-state atoms to the two metastable states. The resonance discharge lamp allows the separation of the 2^1S_0 and 2^3S_1 metastable states. The electric field region modifies the decay rate of the 2^1S_0 state, and consequently changes the number of 2^1S_0 metastables reaching the detector. The number of 2^1S_0 atoms arriving at the detector in specific velocity intervals with the electric field on is compared to the number with the field off to determine the quenching constant k of the 2^1S_0 state.

The vacuum system is constructed of stainless steel and, following bakeout, a pressure in the electric field region of 1×10^{-8} Torr is easily obtainable with liquid-nitrogen trapping. Immediately following the source chamber is a buffer chamber; both are pumped by 2000-liter/sec oil diffusion pumps. The chamber containing the electric field plates is pumped at each end by a 500-liter/sec liquid-nitrogen-trapped pump, while the detector chamber is pumped by a 1000-liter/sec diffusion pump.

Stainless steel plates, each with a 0.65-cm diameter axial hole, separate the various chambers and serve as collimators; additional

0.60-cm diameter collimators are attached to either end of the electric field plates. The maximum beam size at the detector in the worst possible situation is 0.75 cm. The maximum solid angle subtended by the beam is 5×10^{-5} sr and indicates that the number of uv photons reaching the detector from the quench region is negligible in comparison to the metastable beam. The major components will now be described in more detail.

A. Source

Commercial-grade helium is stored in a 10-liter ballast volume at atmospheric pressure, and the gas flow from this reservoir to the source assembly is controlled by a needle valve. A typical flow rate is 0.1 liter/h and is very stable during a 12-h run.

The source assembly consists of a liquid-nitrogen-cooled heat exchanger; a 15-cm long copper tube is attached to this heat exchanger to bring the cooled gas to the beam axis. At the end of this tube, the cooled helium gas effuses from a slit, 0.025-cm wide and 0.5-cm long, oriented parallel to the direction of the tube. The pressure in the source tube is about 0.05 Torr for the flow rate of 0.1 liter/h.

B. Metastabilizer

Ground-state helium atoms are excited to the 2^1S_0 metastable state by electron bombardment immediately after the source slit. The sheath electrode gun is a type described previously.[19] The atomic beam passes antiparallel to the electron beam through a 2-cm long × 0.25-cm wide slot in the collector and then between the two sheath electrodes which define the 1-cm long excitation region. The electron beam originates from a 2.5-cm long, 0.025-cm diameter thoriated tungsten filament heated by about 8A of 3-kHz audio-frequency current; about 20 mA of emission current are obtained at 50 V. A 300-G magnetic field from a concentric solenoid helps focus the electrons onto the collector and confine them to the excitation region. The current through the solenoid is pulsed in conjunction with the electron gun voltage to reduce the duty cycle for heating.

C. Quench Lamp

An air-cooled rf-discharge helium lamp is located adjacent to the first buffer chamber and illuminates the metastable beam through a Pyrex window. The lamps are made from a 9-cm long, 0.8-cm diameter Pyrex tube. The lamps are evacuated and baked before filling to about 5 Torr. A 50-W, 70-MHz oscillator drives the lamp.

D. Electric Field Plates

The electric field region consists of polished aluminum plates 50.8-cm long, 7-cm wide, and maintained at a separation of 1.008 ± 0.001 cm by 1-cm diameter quartz spacers spaced along the edge every 12 cm. Attached to the grounded plate 3 cm from the ends of the high voltage plate are 0.6-cm diameter collimators; they restrict the metastable beam to the central portion of the electric field region. The plates will sustain up to 40 kV/cm.

The electric field is modulated on-off using four parallel 6BK4 triodes as a grounding switch; a 20 megohm resistor protects the HV power supply. An additional 20 megohm resistor and four parallel 6BK4's are modulated with opposite phase to present a constant load to the HV supply. The capacitance of the plates plus HV cable limits the switching time to about 0.1 sec.

The voltage applied to one electric field plate is measured with a 100 megohm, 10^4:1 precision voltage divider, a voltage-to-frequency converter, and a crystal controlled frequency counter. An accuracy of 0.1% is easily obtainable with a sampling time of 0.1 sec.

E. Detection System

The goal of the detection system is to preferentially detect the metastable atoms and to store the data according to time of flight. The electron ejected when a metastable atom strikes the tantalum detector target is focused onto the first dynode of an electron multiplier. The resulting pulse is amplified, counted, and then stored in a PDP-8 computer memory location corresponding to its arrival time after the initial electron gun pulse. The digital computer is also programmed to control the solenoid and gun-pulsing circuits, the lamp oscillator, the electric field modulator, the output keypunch, and a display oscilloscope. An interface network matches the digital pulses from the computer to the other equipment.

The timing aspects of the experiment are shown in Fig. 2. A crystal-controlled oscillator supplies the channel advance pulses, which the PDP-8 uses as a reference to determine the proper sequence of events. Channel 0 corresponds to the duration of the electron gun pulse and the creation of a pulse of metastable atoms. Time $t = 0$ is at the center of channel 0. The focusing solenoid is pulsed on a few milliseconds before channel 0 and is turned off at the end of the gun pulse. To improve the lamp's stability while data counts are being collected, the lamp is turned on or off at the beginning of a 16-msec waiting period. This period is the time the computer needs for adding data collected in buffer registers to that already stored from previous sweeps. After a few hundred lamp on-off data collection cycles with the electric field off (on), the field is switched on (off) and the same number of lamp on-off cycles repeated. To allow the electric field to stabilize, there is about a 1 sec waiting period before data collection resumes after the voltage is switched.

V. DATA ANALYSIS

As displayed by the interface oscilloscope, an example of the data collected and stored by the computer during a run is shown in Fig. 3; the first two time-of-flight distributions correspond, respectively, to lamp off and lamp on with the electric field off, while the last two correspond to lamp off-on with the field on. The display has 100 44.25-μsec wide channels for each time-of-flight distribution and represents the sum of 10^6 separate data collection cycles during a total time of about 12 h. The vertical scale is about 10^5 counts/cm and the total number of metastable atoms counted is about 10^8.

After being punched onto computer cards, the four time-of-flight distributions are analyzed to determine the 2^1S_0 metastable state quenching constant. The first step in the analysis is to obtain the distribution of 2^1S_0 atoms by subtracting for both electric field off and field on the distribution for lamp on from that with the lamp off. Since the background counts are the same for lamp on as for lamp off, this subtraction channel by channel of the two original distributions eliminates any background from the final 2^1S_0 distribution. The result of this subtraction is illustrated in Fig. 4(a), where the time-of-flight distributions for the 2^1S_0 metastable atoms are plotted for both electric field off and electric field on.

Next, the analysis program obtains the ratio of electric field on data to electric field off data. As shown in Fig. 4(b), a straight line is then least-squares fitted to the natural logarithm of this ratio since, according to Eq. (20), ln R versus time-of-flight t is a straight line. The quenching constant k of the 2^1S_0 metastable state is obtained from the slope of this fitted line. The straight line is fitted only between data points that have a number of counts at least 10% of the number in the peak.

VI. RESULTS

A. Systematic Effects

During the course of the experiment, numerous parameters were varied in an attempt to discover any possible systematic error. Within the final accuracy of the experiment, no systematic effect was observed when (1) the background pressure in the electric field region was varied from 10^{-7} to 10^{-8} Torr, (2) the rf-discharge lamp intensity was reduced by 20%, (3) the electron gun voltage was changed from 50 to 100 volts, or (4) the count rate was increased by a factor of two. Moreover, the same quenching constant was obtained both for an electric field $E = 20.00$ kV/cm and for $E = 28.28$ kV/cm. Lack of a systematic lamp intensity effect lends support to the previous assertion that the quenching constant measurement is independent of the initial 2^1S_0 velocity distribution; reducing the lamp intensity changes the 2^1S_0 time-of-flight distribution since the lamp quenching factor $f(v)$ appearing in Eq. (19) is velocity dependent. In addition, changing the electron gun voltage not only changes the 2^1S_0 to 2^3S_1 ratio because of different variation of cross section with voltage, but also changes the 2^1S_0 velocity distribution because of a different recoil momentum.

The extremely small solid angle subtended by the detector excludes any significant contribution to the count rate from uv quench photons originating from either the lamp region or the electric field region. In addition, beam deflection due to the inhomogeneous fringing field of the electric field plates as well as the effect of gravity can be shown to be negligible.

However, one systematic effect, related to the alignment of the source and the electric field plates, was found. Deliberate misalignment could give almost a 1% variation in the measured quenching constant. The explanation is that the effective length of the electric field region is longer than the measured length because of the fringing field at the ends of the field plates. Furthermore, as shown in the appendix, this effective length depends upon the position of the metastable beam with respect to the center of the field plates. After correction for this variation, the measured values of the quenching constant obtained under different alignment conditions agree to within the accuracy of the experiment.

B. Error

Compared to the error arising from the uncertainty in the effective length of the electric field region, the statistical error and also the error in the measurement of the electric field are sufficiently small that they do not contribute. The necessary correction to the length of the electric field region is calculated in the appendix; for the metastable beam passing through the center of the electric field plates, i.e., ideal alignment, the effective length is 2% longer than the measured length. This calculation, which was confirmed by a potential plot in an electrolytic tank, is estimated to be correct to at least ± 25%. Therefore, the error in the length of the electric field region, and consequently the error in the quenching constant k , is ± 0.5%.

C. 2^1S_0 Quenching Constant

The final result for the 2^1S_0 quenching constant is based on the weighted average of 43 12-h runs at 20.00 kV/cm and 66 12-h runs at 28.28 kV/cm for He^4, and 20 12-h runs at 28.28 kV/cm for He^3. A consideration of the error in the effective length of the electric field region gives a final value of k = 0.933 ± 0.005 for the quenching constant of the 2^1S_0 metastable state of helium. This result, essentially the same for both He^3 and He^4, is in good agreement with the theoretical values of Jacobs[5,17] (k = 0.931) and of Drake[18] (k = 0.932), and also with an earlier experimental value[11] (k = 0.926 ± 0.020). To the extent that the matrix element used to calculate the quenching constant k is identical to the matrix element required in the calculation of the two-photon decay rate, but with one photon frequency equal zero, the present experiment serves as a test of the two-photon decay matrix element ten times more precise than the previous measurement[1] of the 2^1S_0 metastable state lifetime.

ACKNOWLEDGEMENTS

The assistance of Professor Howard Shugart in programming the PDP-8 computer is greatly appreciated. Dr. Verne Jacobs kindly furnished his unpublished value for $\sum_n M_n(0)$, while Professor Gordon Drake furnished the results of his calculation of the quenching constant prior to publication. Finally, discussions with Professor Willis Lamb, Jr., Charles Schwartz, Ken Lea, and Peter Fontana regarding the theory of quenching of a metastable state by an electric field were very informative.

APPENDIX: FRINGING FIELD

The two-dimensional solution for the electric field produced by two parallel plates (see Fig. 5), one infinite and the other semi-infinite, a distance h apart is obtained from the transformation[20]

$$z = \frac{h}{\pi}\left(\exp\left(\pi \frac{W}{V_o}\right) + \pi \frac{W}{V_0} + 1\right)$$

with

$$z = x + iy \quad \text{and} \quad W = U + iV .$$

Thus,

$$x = \frac{h}{\pi}\left[\exp\left(\pi \frac{U}{V_o}\right)\cos\left(\pi \frac{V}{V_o}\right) + \pi \frac{U}{V_o} + 1\right]$$

and

$$y = \frac{h}{\pi}\left[\exp\left(\pi \frac{U}{V_o}\right)\sin\left(\pi \frac{V}{V_o}\right) + \pi \frac{V}{V_o}\right] .$$

The electric field E is

$$E = \left|\frac{dW}{dz}\right| = \frac{V_o}{h\left|\exp\left(\pi \frac{U}{V_o}\right)\cos\left(\pi \frac{V}{V_o}\right) + 1 + i\exp\left(\pi \frac{U}{V_o}\right)\sin\left(\pi \frac{V}{V_o}\right)\right|}$$

or,

$$E^2 = \frac{\left(\frac{V_o}{h}\right)^2}{\exp\left(2\pi \frac{U}{V_o}\right) + 2\exp\left(\pi \frac{U}{V_o}\right)\cos \pi \frac{V}{V_o} + 1} .$$

If a particular value of y is chosen, then the solutions for E^2 versus x with V as a parameter can be obtained, as shown in Fig. 5. A numerical integration of E^2 along x gives the effective value of

E^2 experienced by a metastable atom passing through the electric field plates. Conversely, if E^2 is taken as the value obtained from the measured values of V_o and h, then the field plates can be considered to have an effective length $L + 2\delta$ where L is the measured length. For $y = \frac{1}{4} h$, $\delta = 0.35\ h$, while for $y = \frac{1}{2} h$, $\delta = 0.46\ h$, and for $y = 3/4\ h$, $\delta = 0.70\ h$.

References

* Work supported by U. S. Atomic Energy Commission.

1. R. S. Van Dyck, Jr., C. E. Johnson, and H. A. Shugart, Phys. Rev. A4, 1327 (1971).
2. G. Breit and E. Teller, Astrophys. J. 91, 215 (1940).
3. W. Zernik, Phys. Rev. 132, 320 (1963); 133, A118 (1964).
4. G. W. F. Drake, G. A. Victor, and A. Dalgarno, Phys. Rev. 180, 25 (1969).
5. V. Jacobs, Phys. Rev. A4, 939 (1971).
6. Li^{+}: M. H. Prior and H. A. Shugart, Phys. Rev. Letters 27, 902 (1971); Ar^{16+}: R. Marrus and R. W. Schmieder, Phys. Rev. A5, 1160 (1972).
7. Li^{2+}: C. Y. Fan, M. Garcia-Munoz, and I. A. Sellin, Phys. Rev. 161, 6 (1967); C^{5+}: D. E. Murnick, M. Leventhal, and H. W. Kugel, Phys. Rev. Letters 27, 1625 (1971); O^{7+}: M. Leventhal, D. E. Murnick, and H. W. Kugel, Phys. Rev. Letters 28, 1609 (1972) and G. P. Lawrence, C. Y. Fan, and S. Bashkin, Phys. Rev. Letters 28, 1612 (1972).
8. W. E. Lamb, Jr., and R. C. Retherford, Phys. Rev. 79, 41 (1950).
9. C. E. Johnson, Bull. Am. Phys. Soc. 17, 454 (1972).
10. H. K. Holt and R. Krotkov, Phys. Rev. 144, 82 (1966).
11. R. Petrasso and A. T. Ramsey, Phys. Rev. A5, 79 (1972).
12. P. R. Fontana and D. J. Lynch, Phys. Rev. A2, 347 (1970).
13. H. K. Holt and I. A. Sellin, Phys. Rev. A6, 508 (1972).
14. L. I. Schiff, Quantum Mechanics (McGraw-Hill, New York, 1955), pp. 254 f.
15. M. Goeppert-Mayer, Ann. Physik 9, 273 (1931).

References (Continued)

16. Ref. 14, pp. 201 - 204.

17. V. Jacobs (private communication).

18. G. W. F. Drake, Can. J. Phys. (to be published).

19. F. M. J. Pichanick, R. D. Swift, C. E. Johnson, and V. W. Hughes, Phys. Rev. 169, 55 (1968).

20. J. Jeans, Mathematical Theory of Electricity and Magnetism, 5th edition (Cambridge University Press, Cambridge, England, 1960), p. 275.

FIGURE CAPTIONS

Fig. 1. Apparatus outline. Ground-state atoms effuse from the source and are excited to the 2^1S_0 and 2^3S_1 metastable states by electron bombardment. The rf-discharge lamp quenches the 2^1S_0 state. After passing through the electric field region, metastable atoms are detected by electron ejection from a metal target.

Fig. 2. Timing scheme. Channel advance pulses determine the channel width and furnish synchronous pulses for control of the electron gun, solenoid, lamp, and electric field. The lamp is switched on-off for alternate data collection cycles; the electric field is also switched every few hundred cycles.

Fig. 3. Interface oscilloscope display. The first half of the display, consisting of 100 44.25-μsec wide channels for both lamp off and on, corresponds to the electric field off, while the second 200 channels are with the field on. The vertical scale is about 10^5 counts/cm.

Fig. 4(a). Time-of-flight distributions. The upper 2^1S_0 distribution is with the electric field off, while the lower is with the field on; the decrease in height represents quenching by the electric field. (b). ln plot. The ratio of the two distributions versus time-of-flight is a straight line on a logarithmic plot. The quenching constant k is obtained from the slope of the least-squares fitted straight line; the fit only includes points which have counts equal to at least 10% of the number in the peak of the distribution.

Fig. 5. Fringing field. The square of the electric field produced by two parallel plates is plotted versus x for two separate values of y . The end of the high voltage plate is at $x = 0$, while the infinite plate coincides with $y = 0$.

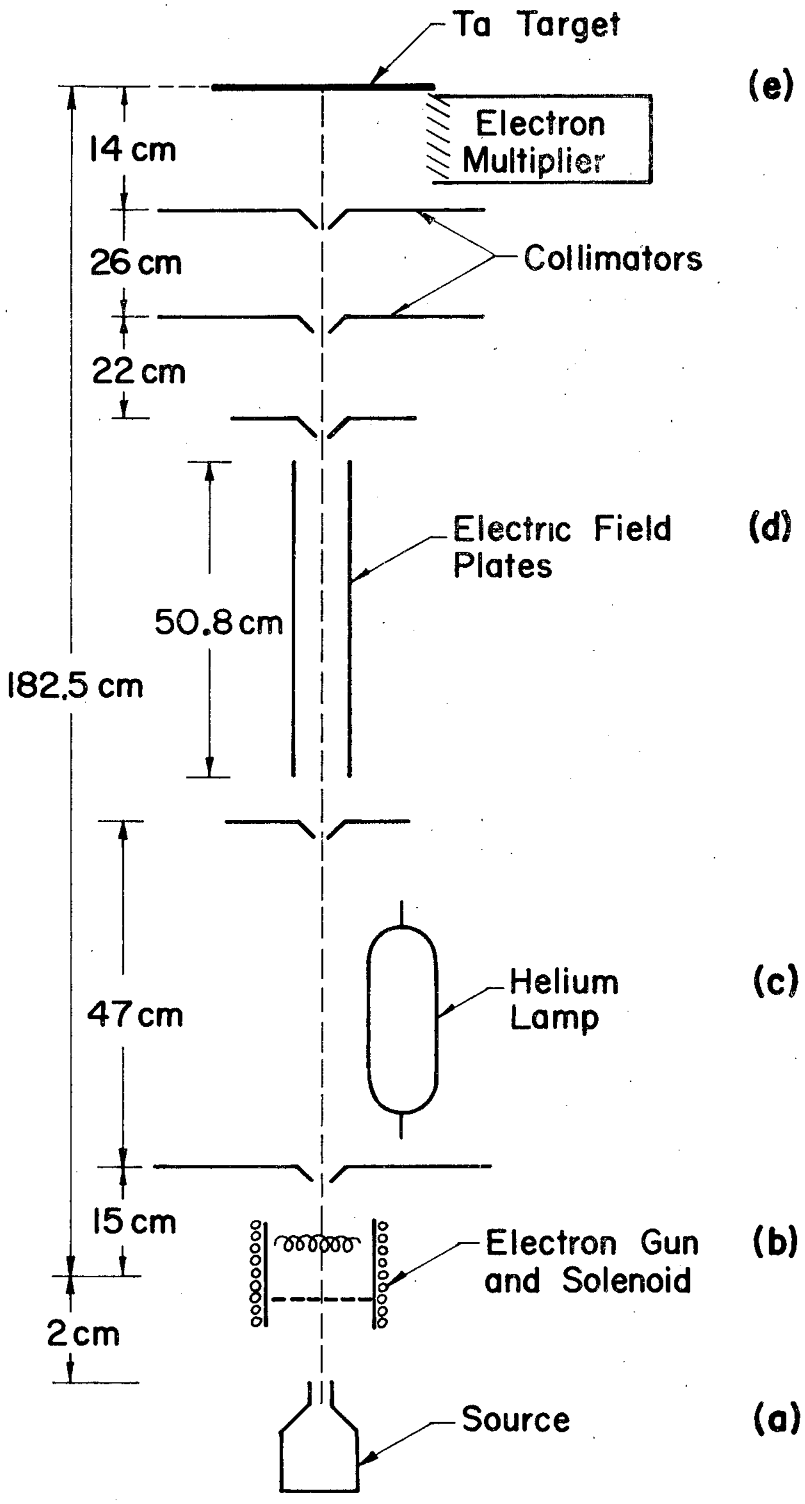

XBL 724-752

Fig. 1

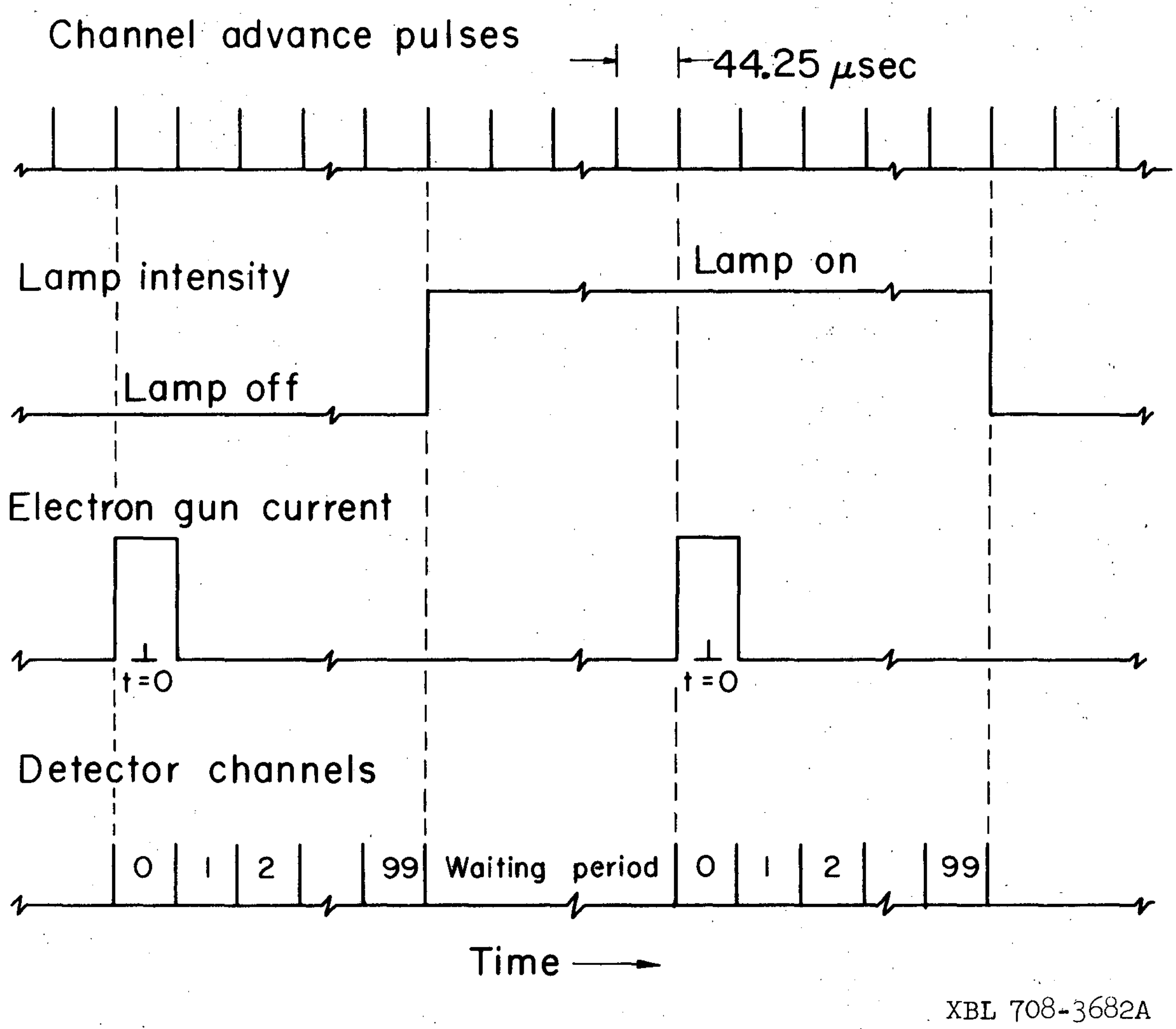
Channel advance pulses
44.25 μsec
Lamp intensity
Lamp on
Lamp off
Electron gun current
t=0
t=0
Detector channels
0
1
2
99
Waiting period
0
1
2
99
Time
XBL 708-3682A

Fig 2

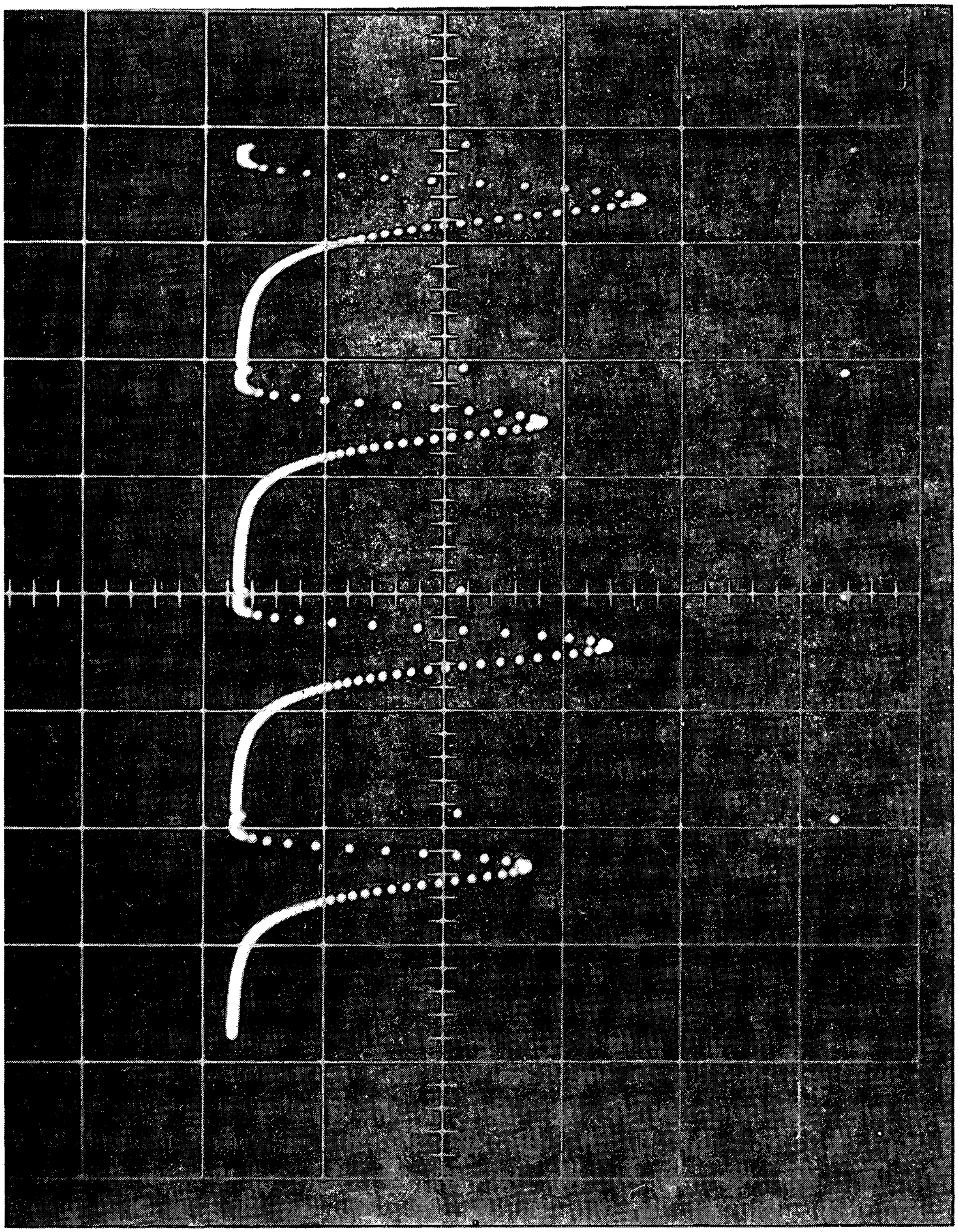

XBB 7210-5360

Fig. 3

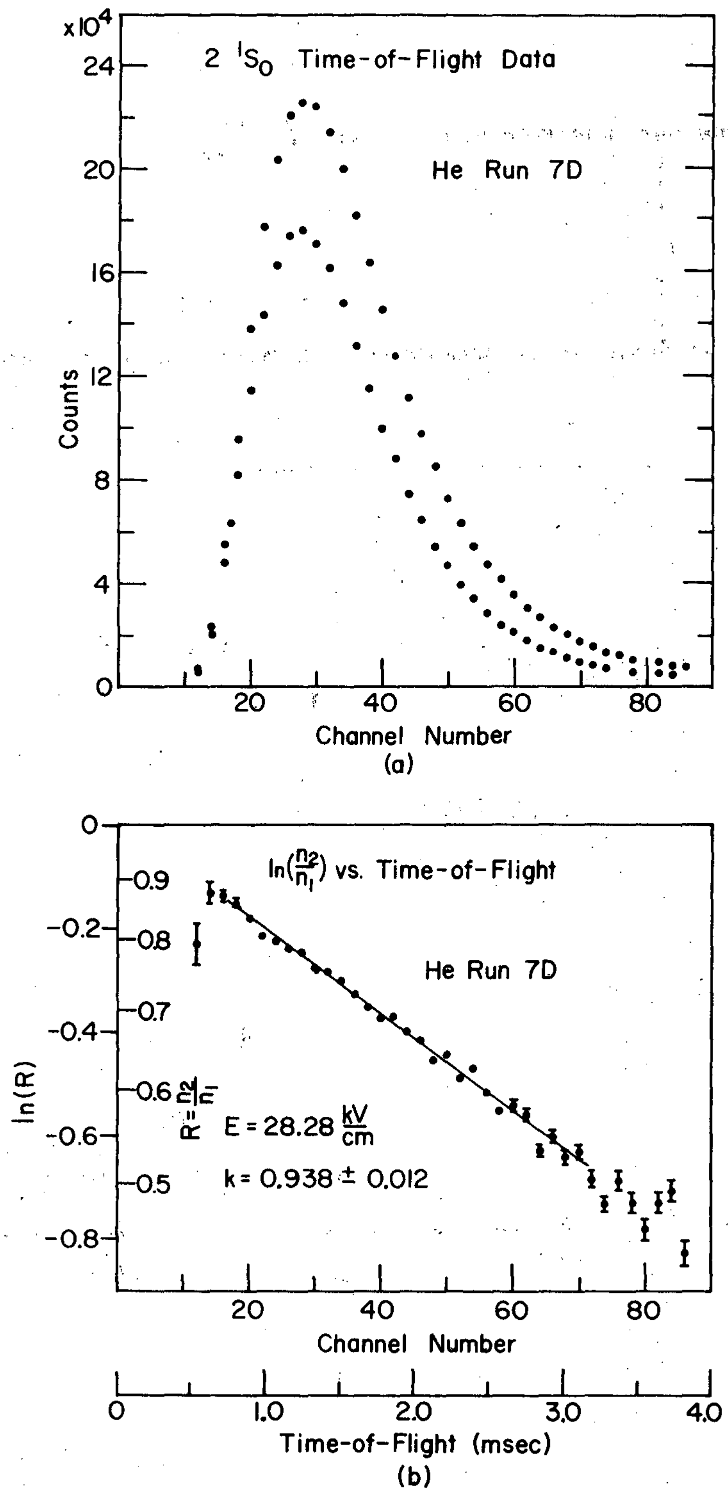

XBL 725-814

Fig. 4

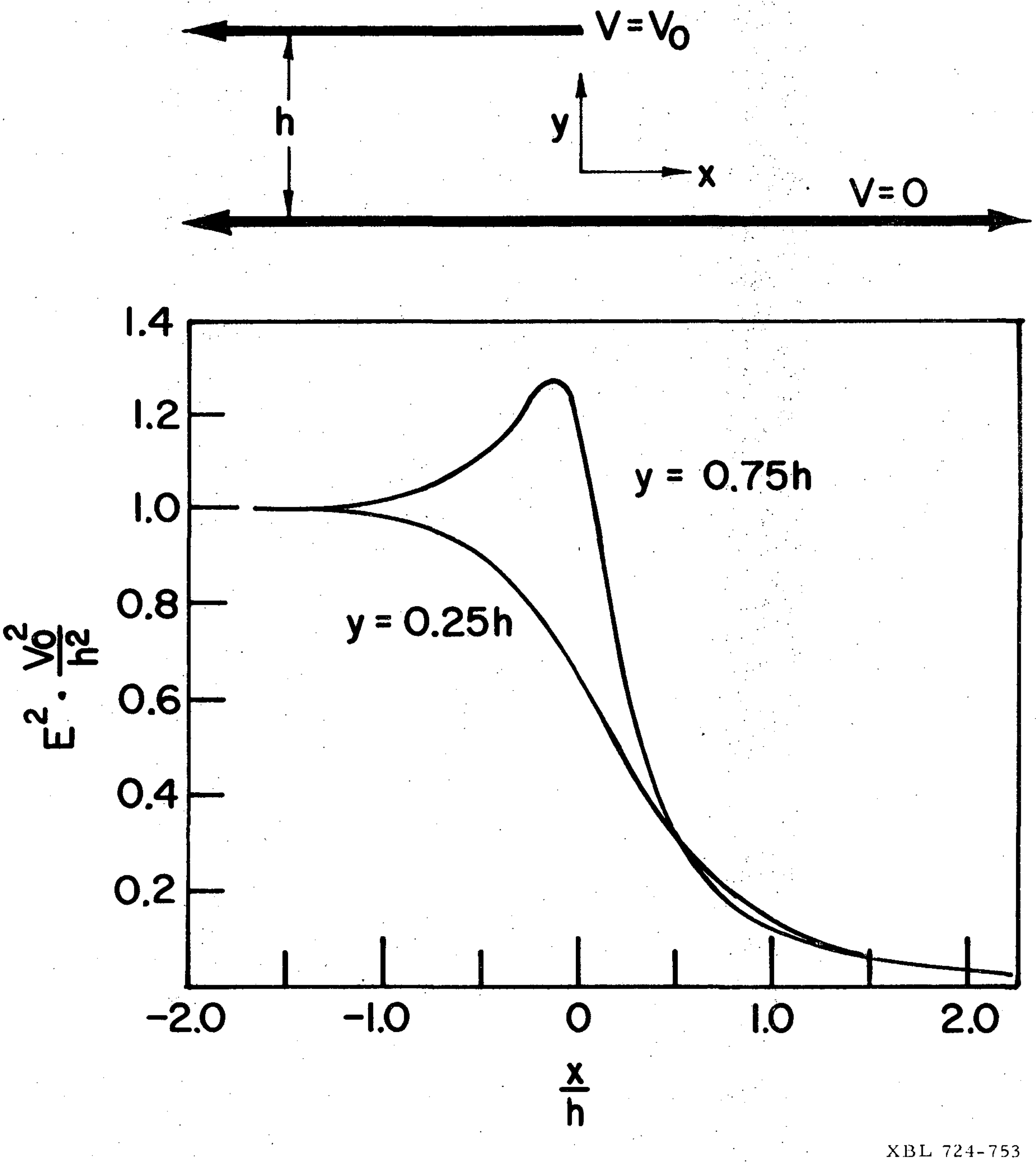

XBL 724-753

Fig. 5

TECHNICAL INFORMATION DIVISION
LAWRENCE BERKELEY LABORATORY
UNIVERSITY OF CALIFORNIA
BERKELEY, CALIFORNIA 94720